Bone architecture adaptations after spinal cord injury: impact of long-term vibration of a constrained lower limb

S. Dudley-Javoroski[1], **M. A. Petrie**[1], **C. L. McHenry**[1], **R. E. Amelon**[2], **P. K. Saha**[2,3], and **R. K. Shields**[1]

R. K. Shields: richard-shields@uiowa.edu

[1]Department of Physical Therapy and Rehabilitation Science, Carver College of Medicine, The University of Iowa, 1-252 Medical Education Building, Iowa City, IA 52242, USA

[2]Department of Electrical and Computer Engineering, The University of Iowa, Iowa City, IA, USA

[3]Department of Radiology, Carver College of Medicine, The University of Iowa, Iowa City, IA, USA

Abstract

Summary—This study examined the effect of a controlled dose of vibration upon bone density and architecture in people with spinal cord injury (who eventually develop severe osteoporosis). Very sensitive computed tomography (CT) imaging revealed no effect of vibration after 12 months, but other doses of vibration may still be useful to test.

Introduction—The purposes of this report were to determine the effect of a controlled dose of vibratory mechanical input upon individual trabecular bone regions in people with chronic spinal cord injury (SCI) and to examine the longitudinal bone architecture changes in both the acute and chronic state of SCI.

Methods—Participants with SCI received unilateral vibration of the constrained lower limb segment while sitting in a wheelchair (0.6*g*, 30 Hz, 20 min, three times weekly). The opposite limb served as a control. Bone mineral density (BMD) and trabecular micro-architecture were measured with high-resolution multi-detector CT. For comparison, one participant was studied from the acute (0.14 year) to the chronic state (2.7 years).

Results—Twelve months of vibration training did not yield adaptations of BMD or trabecular micro-architecture for the distal tibia or the distal femur. BMD and trabecular network length continued to decline at several distal femur sub-regions, contrary to previous reports suggesting a "steady state" of bone in chronic SCI. In the participant followed from acute to chronic SCI, BMD and architecture decline varied systematically across different anatomical segments of the tibia and femur.

Conclusions—This study supports that vibration training, using this study's dose parameters, is not an effective antiosteoporosis intervention for people with chronic SCI. Using a high-spatial-

---

Correspondence to: R. K. Shields, richard-shields@uiowa.edu.

resolution CT methodology and segmental analysis, we illustrate novel longitudinal changes in bone that occur after spinal cord injury.

Keywords

Bone mineral density; Osteoporosis; Spinal cord injury; Trabecular architecture; Vibration

Introduction

Spinal cord injury (SCI) precipitates severe bone loss of the paralyzed limbs through a combination of mechanical, neural, and hormonal factors [1]. Bone mineral density (BMD) is lost most rapidly in the initial post-SCI phase, with initial rates as high as 4.7 % per month [2]. BMD losses can exceed 34% by 1 year and 52 % by 4 years [3]; however, we have limited understanding of the concurrent trabecular architectural changes that occur. There is a need for novel antiosteoporosis rehabilitation therapies as well as more detailed methods to assess bone architecture after SCI.

Rehabilitation strategies for post-SCI bone often use exogenous mechanical loading to subsidize the mechanical loads lost from muscle contraction and weight bearing. The precise combination of mechanical stimuli required to preserve bone architecture after SCI is unknown. Because the cellular and molecular response to mechanical stimulation is incompletely understood, numerous modes of input are viable candidates for osteo-regulatory signals. High-magnitude compressive forces generated by electrical muscle stimulation attenuate BMD decline for individuals with recent SCI [4–7]. However, patients with long-term SCI and osteoporosis may be poor candidates to receive high-magnitude muscle loading interventions [8]. Moreover, patients with lower motor neuron injury (peripheral nerve damage) cannot electrically activate their limbs with standard commercially available electrical stimulators [9]. For the large population of patients with chronic SCI and/or lower motor neuron involvement, an alternate approach is needed for preserving bone architecture after SCI.

Low-intensity, usually imperceptible vibratory loads predominate bone's daily strain history [10]. Thus, in the absence of postural contractions after SCI, osteoporosis may develop in part because pervasive low-magnitude strains are lost. Animal studies support that low-magnitude vibratory loads are anabolic to bone. Low-magnitude vibratory input (0.25–$0.3g$) yielded improvements in bone formation rate [11], bone turnover biomarkers [12], bone architecture [11], and mechanical stiffness [13]. In sheep femora, 12 months of hindlimb vibration training (30 Hz, $0.3g$) yielded a 34 % difference in trabecular BMD between experimental animals and controls [14]. The 30-Hz vibratory stimulus in that study falls within the frequency spectrum of volitional muscle contraction [15]. As noted above, small-amplitude loads in the frequency spectrum of volitional muscle contraction comprise the overwhelming majority of bone's daily load exposure [10]. While these experiments do not negate the considerable evidence for the osteogenic potential of large compressive loads [4–7], they do support that small oscillatory loads can subsidize lost mechanical strains after SCI. If this is indeed true, a new therapeutic avenue may exist for people with SCI who

cannot activate paralyzed muscle (due to lower motor neuron lesion) or who cannot receive large-magnitude muscle loads (due to advanced post-SCI osteoporosis).

Several studies of vibratory loading in humans with SCI have used whole-body vibration (WBV), in which the participants stand atop a vibrating platform [16–18]. The two studies which included bone assessments showed no effect of WBV training on BMD or trabecular micro-architecture [17, 18]. Given the strong evidence for the anabolic potential of vibration from animal studies, we were surprised by these findings. Therefore, we designed an experimental apparatus to administer a carefully controlled dose of vibration at a known compressive load in a way that more closely replicates the mechanical loading conditions of several successful animal studies [11, 13]. In this system, participants with SCI receive low-intensity vibration to a constrained lower limb segment from a seated position, rather than in standing through passive weight bearing [19], allowing the opposite limb to serve as a within-subject control.

The observation that bone density incompletely predicts bone strength [2] highlights the complementary role played by other factors such as bone tissue quality [20] and bone architecture [21]. Several cross-sectional studies confirmed that trabecular architecture is markedly deteriorated after chronic SCI [22]. The only available longitudinal studies described changes of bone stiffness and strength properties over a short-time post-SCI but did not report adaptations of trabecular micro-architectural parameters [2, 23, 24]. Thus, no estimate is currently available for the time course of trabecular architecture degradation after SCI.

The purpose of this report is to determine the effect of a controlled dose of vibratory mechanical input upon individual trabecular bone regions in people with SCI. A secondary purpose is to examine longitudinal bone architecture changes in both the acute and chronic state of SCI. The high-resolution CT imaging technique used in this report offers an unprecedented level of resolution for measuring in vivo skeletal adaptations in human patients in order to determine the efficacy of vibratory input for enhancing bone integrity after SCI.

Methods

Participants

The protocol was approved by the University of Iowa Human Subjects Institutional Review Board. Informed consent was obtained from all individual participants included in the study. Forty-two individuals with motor-complete SCI (American Spinal Injury Association (ASIA) Impairment Scale (AIS) A and B) [25] and 21 individuals without SCI underwent peripheral quantitative computed tomography (pQCT) imaging to establish benchmarks to aid interpretation of the study outcomes. A portion of these participants appeared in a previous report [3]. These individuals ranged from 0.1 to 29.2 years post-SCI (mean 5.9 years). Six individuals with chronic paralysis participated in the longitudinal vibration training component of this study (Table 1). Using estimates of variation obtained from pilot individuals with chronic SCI, statistical power exceeded 0.825 to detect an effect size of 10 % with six participants. Exclusion criteria were thyroid disorder, previous fracture at the

scan sites, medications known to affect bone metabolism, a history of bone pathology, and pregnancy.

pQCT imaging

pQCT measurements were performed with a Stratec XCT3000 densitometer (Stratec Medical, Pforzheim, Germany). Voxel size was 0.4 mm^3, scanner speed was 25 mm/s, and slice thickness was 2.2 mm. pQCT images were obtained at 4 % of tibia length and 12 % of femur length (measured from the distal end). Single pQCT slices were analyzed for trabecular BMD using our standard method [3, 4, 6, 26]. Participants with SCI underwent between one and six bilateral pQCT scans spanning as much as 8.9 years post-SCI. Non-SCI participants underwent a single bilateral pQCT scan.

High-resolution CT

One individual underwent CT imaging at 4 months and at 2.7 years post-SCI (participant 1). Six other participants underwent CT scanning before and after receiving 12 months of vibration training (details below). Bilateral limbs were imaged via high-resolution multi-detector CT (Definition Flash, Siemens Healthcare, Erlangen, Germany) and the INTable™ Calibration Phantom Couch Pad. The single-source spiral acquisition used 16×0.3-mm detector collimation, 120 kVp, 240 mAs, 1.0 pitch, and a gantry rotation speed of 1.0 s. Helical scanning was performed to obtain 0.4-mm slices, which were then reconstructed at 0.3 mm using a normal cone beam method with a U70u kernel to achieve high structural resolution. Scan time was approximately 10 min. An investigator registered the right and left limbs and defined six uniform axial regions spanning the most distal 4–16 % of the tibiae and femora (2 % per segment) (Fig. 1a). This enabled us to determine whether adaptations differed along the longitudinal axis of the bone. Our previous work indicated that adaptations to SCI and to mechanical loading interventions may also vary in different regions of the bone cross section [5, 26].We applied a set of four radial peel modes to separately analyze the central and peripheral zones of the bone cross section (Fig. 1a). The first three peel modes concentrically removed 30, 45, and 60 % of voxels from the trabecular envelope. The final peel mode ("peripheral") analyzed the outermost ring of the trabecular envelope by subtracting the 60% peel area from the 30 % peel area. These four analysis approaches enabled us to determine whether adaptations differed across the bone's cross section.

The investigator who analyzed the CT images was kept blinded to the training status of the participants. Images were processed using volumetric topologic analysis (VTA) [27]. Trabecular BMD was calculated as the average physical density for each region. Trabecular surface width (SW, μm) was calculated as the BMD-weighted average surface width for each region. Trabecular thickness (THK, mm) was calculated as the BMD-weighted average surface thickness for each region. Network length (NL) was found by dividing the number of surface voxels in the trabecular lattice by the number of voxels in the volume of interest. It is unitless, as it is the ratio of the trabecular volume to the total volume considered. Other key architectural parameters relied upon the VTA classification of trabecular elements as plate-like and rod-like structures. Osteoporotic bone typically displays evidence of erosion of plates and conversion to rods [28]. Plate volume fraction (PVF) represents the relative

preponderance of plates in a volume, weighted to BMD. Surface-to-curve ratio (SCR) is an index of relative "plateness" compared to "rodness" of a trabecular region [27]. A low SCR indicates extensive erosion of plates and conversion to rods, a process known to occur in osteoporosis [28].

Vibration intervention

Participants received vibration to the constrained limb segment while sitting in a wheelchair (Fig. 1b). One limb remained untrained as a within-subject control. The trained leg was the dominant limb for three participants and the non-dominant limb for the other three individuals. The linearity, repeatability, accuracy, and transmissibility of vibration for this system have been previously described [19]. A compressive pre-load of 10–15% of body weight (%BW) was applied to the top of the knee to couple the limb segment to the vibrating surface, after which a cyclical load of 35 % of body weight was applied (5 s on and 10 s off) during the continuous vibration. This was done to facilitate transmissibility of the vibratory stimulus and to mimic weight-bearing conditions carried out in previous animal experiments. We have previously demonstrated that this low level of compressive load does not independently trigger bone adaptations in paralyzed humans [6]. The vibration system delivered vertical oscillations of $0.6g$ at 30 Hz for 20 min. These parameters were selected to reflect the vibration conditions of recent studies that reported anabolic effects of vibration in the murine tibia [11, 13, 29]. We previously verified that vibration using these parameters does not increase background EMG activity [30] and downregulates monosynaptic reflex activity [31]. Reflex-mediated muscle contractions did not occur, eliminating muscle force as a potential confounding source of mechanical load to the bone. Participants were asked to complete three vibration sessions per week.

Statistical analysis

We used a repeated-measures two-way (training×time) analysis of variance (ANOVA) to analyze pQCT-derived BMD. We analyzed CT data in three ways. First, because of the complexity of the CT data (six analyzed regions and four peel modes per region, per dependent variable), we conducted initial statistical analyses using the mean value for all six sampled CT regions. We used a repeated-measures two-way (training×time) ANOVA for each dependent variable: BMD, SW, THK, NL, PVF, and SCR, with follow-up tests (Tukey) as indicated. Secondly, when the above two-way ANOVA indicated a significant training×time interaction for the mean CT data, we inspected each individual CT segment to determine which regions were most responsive to training. To accomplish this, we performed two-way repeated-measures (training×time) ANOVAs on raw data for each such segment. Thirdly, we conducted a final series of ANOVA tests on normalized data. For each dependent variable, we converted the 12-month data point to a percent of the baseline value and performed a two-way (training×region) repeated-measures ANOVA. All analyses were adjusted for experiment-wise error. Alpha was set to $p=0.05$.

Results

Compliance for the vibration training participants with the recommended dose of training (three sessions per week) was 76.9 % over 12 months of training (Table 1).

For pQCT-derived BMD, no significant interaction existed between training and time for either the tibia or the femur. A significant main effect of limb existed for tibia BMD ($p=0.034$). Follow-up testing revealed that BMD of the trained limb was significantly higher than the untrained limb at both the pre-training and post-training conditions. Because an equal number of dominant and non-dominant limbs received the training stimulus, this offset at baseline appears to reflect a random variation effect. Thus, pQCT analysis showed no evidence of training-related adaptations in BMD for the vibration cohort.

CT-derived BMD and architecture values processed using a 30 % peel method illustrate the strict measurement strategies employed in this study (Fig. 2). For the tibia (using the mean of all CT regions), a significant training×time interaction occurred for two conditions: BMD processed with the 30% peel ($p=0.041$) and THK processed with the 60% peel ($p=0.038$). Follow-up testing revealed a significant difference in BMD between limbs at the baseline measurement ($p=0.048$), consistent with the pQCT analysis. A significant difference also existed for THK between the baseline and 12-month assessments for the untrained limb only ($p=0.004$). For these two conditions, we then proceeded to examine each separate CT region individually. No significant training×time interaction emerged for any CT region for THK. For BMD, a significant interaction existed for CT region 10 (spanning 10–12 % of tibia length) ($p=0.046$). However, follow-up tests indicated no pairwise effects for time or training.

Considering the differences in baseline between limbs, we analyzed normalized CT data (percent of baseline) for each dependent variable. A significant training×region interaction existed for one condition: NL processed with the "peripheral" peel ($p=0.018$). For region 5 (12–14% tibia length), untrained limb-normalized NL was significantly greater than trained limb-normalized NL ($p=0.007$). Taken together, this detailed analysis using CT uncovered no evidence for a training effect for the vibration intervention at the distal tibia.

CT-derived BMD and architecture values for the femur appear in Fig. 2. Using the mean of all CT regions, a significant training×time interaction emerged for only one condition: SCR processed with the 45 % peel ($p=0.026$). However, this interaction did not persist for any of the CT regions when examined individually. For the normalized femur CT data (percent of baseline), a significant training×region interaction emerged for five conditions: SCR processed with the "peripheral" peel; NL processed with the 30 %, 45 %, and peripheral peels; and PVF processed with the peripheral peel (interaction $p=<0.001, <0.001, 0.027, 0.020,$ and 0.003, respectively). Pairwise tests showed trained versus untrained limb differences at several of the individual CT regions. However, the between-limb difference occurred in the hypothesized direction (trained limb>untrained limb) in only one instance: NL processed with the 30 % peel at region 12 ($p=0.003$). Thus for the distal femur normalized data, CT uncovered evidence for a training effect of vibration for only one architecture variable at just one CT region processed via one peel mode. Taken together, there was no compelling evidence that vibration training triggered BMD or architecture changes at the distal femur.

Chronic SCI BMD and architecture

Most [3, 32, 33] but not all [34] previous studies have indicated that bone loss reaches a steady state after SCI, usually between 4 and 8 years. pQCT data from the vibration cohort support this view: no decline in pQCT-derived BMD occurred over 12 months for the tibia (p=0.229) or the femur (p= 0.176). However, this issue has not been investigated using high-resolution CT imaging nor has the possibility of a steady state been examined for trabecular micro-architecture parameters. Based on the absence of training-related differences between limbs (as described above), we pooled the trained and untrained limbs for all 30 % peel BMD and architecture variables and analyzed differences between the baseline and 12-month time points. At the distal tibia, BMD and NL declined significantly across time (p<0.001, p=0.016, respectively), indicating that these parameters had not achieved steady state. Across all CT regions, mean percent decline was 24.3 % for BMD and 14.4 % for NL. No individual CT region experienced a significant decline in BMD or NL over 12 months (all p>0.05). At the distal femur, pooled-limb BMD and NL likewise declined significantly across time (p<0.001, p=0.003, respectively). Across all CT regions, mean percent decline was 29.5 % for BMD and 35.5 % for NL. For BMD, individual CT regions 2 and 3 showed significant declines over time (both p<0.047). CT region 2 likewise showed a significant decline in NL over time (p=0.015). Thus, CT imaging enabled us to detect continued declines in BMD and NL at specific anatomical sub-segments that were not detectable with single-slice pQCT imaging.

Acute-to-chronic SCI BMD and architecture

pQCT-derived BMD declined precipitously over time post-SCI for the distal tibia and distal femur (Fig. 3). The single individual who underwent longitudinal CT imaging appears as the red plot in this figure. BMD for this participant declined by 55.9 % at the distal tibia and 73.4 % at the distal femur. This participant's position within the longitudinal pQCT database confirms that his BMD declined in a typical fashion over the first 2.7 years post-SCI. This supports that the participant's micro-architecture changes (analyzed by CT) may be considered generally typical for an individual with SCI progressing from the acute to the chronic stage (Figs. 4 and 5). Representative examples of reconstructed distal tibia images for this participant appear in Fig. 4a. At the distal tibia, BMD declined by an average of 48.1 % over the six sampled regions (Fig. 4b). Region 1, spanning 4–6 % of tibia length, showed the most severe BMD decline (76.7 %). BMD decline was progressively less severe moving toward the most proximal sampled regions. BMD declined by just 14.9 % at region 6, which spanned 14–16 % of tibia length.

Tibia micro-architecture parameters for this participant declined by varying amounts over the first 2.7 years post-SCI (Fig. 4b). Trabecular NL declined by an average of 41.9 % over the six sampled regions, while PVF declined by an average of only 2.5 %. The key unifying feature among tibial architecture parameters was that without exception, the maximal decline occurred in the most distal region (region 1) and the minimal decline occurred in the most proximal region (region 6). Thus, the spatial pattern of trabecular architecture decline for this participant closely paralleled his pattern of BMD decline.

Representative examples of reconstructed distal femur images appear in Fig. 5a. At the distal femur, BMD declined by an average of 53.6 % over the six sampled regions (Fig. 5b). BMD loss in the distal femur was most severe in the central regions, not the distal regions as in the tibia. Region 3, spanning 8–10 % of femur length, showed the most severe BMD decline over 2.7 years (66.3 %). Similar to the tibia, BMD decline was least severe at the most proximal femur region (region 6 38.5 % decline). This pattern of regional decline also existed for femur architecture parameters. The decline of each architecture variable was most severe at the center regions (regions 3 and 4) and least severe at the most proximal region (region 6). Just as in the tibia, femur NL showed the greatest mean decline across time (38.1 %) and PVF showed the least decline (2.9 %).

To summarize, for a participant followed longitudinally for the first 2.7 years post-SCI, the average BMD loss across the entire distal tibia (~48 %) was comparable to the average BMD loss over the entire distal femur (~54 %). Likewise, the magnitude of the decline for each trabecular architecture parameter was similar between the tibia and femur. However, high-resolution CT imaging enabled us to detect spatial differences in the anatomical distribution of BMD/architecture decline between the tibia and femur. BMD and architecture loss were most severe in the ultra-distal tibia, whereas losses for the femur were greatest at the central portion of the epiphysis.

Discussion

The purpose of this study was to determine the effect of a controlled dose of vibratory mechanical input upon individual trabecular bone regions in people with SCI. A secondary purpose was to examine longitudinal bone architecture changes in both the acute and chronic state of SCI. This investigation afforded us a unique opportunity to explore whether a steady state exists for trabecular micro-architecture with chronic SCI, a phenomenon not previously described in the literature.

Outcomes of vibration training

We previously confirmed that the vibration intervention mimicked the mechanical input conditions of previous animal studies [19] and that it did not cause reflexive muscle contractions [30, 31]. We used a novel and sophisticated imaging approach to obtain outstanding imaging resolution for in vivo bone adaptations. Based on results from animal models we anticipated that 12 months of vibration of the constrained limb segment at 0.6*g*, 30 Hz would yield improvements in measures of trabecular BMD and micro-architecture. High-resolution CT imaging yielded no evidence of BMD adaptation and very weak evidence for architecture adaptation: enhanced NL of a single femur region, processed with a single peel mode. The results of this detailed imaging study do not support that long-term vibration training at this particular dose yielded bone adaptations in these participants. As has been reported elsewhere [35], the skeletal system in patients with *chronic* SCI seems to be refractory to change in response to mechanical loading. The findings of this study corroborate and amplify the findings of previous studies showing an unexpected insensitivity of bone to vibratory input in paralyzed human extremities [17, 18].

Previous animal studies used hindlimb unloading to simulate the mechanical load conditions of reduced activity, such as would occur after SCI [11, 13].We are aware of no previous animal or human studies that have intervened with vibration of a constrained limb segment after paralysis. An effective vibration-based intervention could offer patients with chronic SCI and associated osteoporosis a way to address bone loss without risking exposure to high-amplitude mechanical loads. This segment of the SCI patient population currently lacks such an option. In contrast, patients with acute SCI (and near-normal bone status) can readily perform electrical muscle stimulation protocols that restore physiologic levels of mechanical load to the paralyzed skeletal system. When performed at an appropriate dose of compressive load (~150 % of body weight) and in a manner that minimizes shear forces [36, 37], high-force muscle contraction preserves BMD and trabecular architecture longitudinally after SCI [4–7]. We believe that it is possible that individuals with acute SCI could also demonstrate BMD and architecture adaptations in response to vibration training. However, vibration training would not offer these patients the ancillary benefits of routine electrically evoked muscle contractions, namely, improvements in glucose disposal and clinical markers of metabolic function [38–42]. No strong rationale therefore exists for using vibration instead of electrical stimulation training to address bone decline in patients with acute SCI. Individuals with chronic SCI and the subset of acute SCI patients with lower motor neuron damage remain the key potential beneficiaries for such an intervention.

Given the unprecedented level of detail of the CT analysis in the present study, the absence of training effects over 12 months strongly supports that vibration training at the study dose does not trigger anabolism of bone in participants with chronic SCI. Had training effects been present, we are confident that the CT imaging methodology would have possessed sufficient resolution to detect them. This is supported by the sensitivity shown by the CT technique for detecting BMD and architecture change in the individual followed longitudinally from acute to chronic SCI. Further work is needed to determine whether other vibration dose parameters (frequency, amplitude, duration, training volume, etc.) could offer an osteogenic stimulus to bone in patients with long-term SCI.

Longitudinal decline of micro-architecture

Using pQCT, we determined that the bone degradation experienced by participant 1 over 2.7 years post-SCI was generally typical compared to a large SCI cohort (*n*=42). This assured us that his CT-derived BMD and micro-architecture values were not likely to represent spurious outlier values. The uneven spatial distribution of BMD and architecture decline for participant 1 is a novel finding. Single pQCT slices indicated that BMD loss was 55.9 % at the distal tibia and 73.4 % at the distal femur. Multi-slice CT imaging offered greater insight into the spatial distribution of these bone adaptations. BMD losses at the tibia were comparable to those seen with pQCT (~50 %) for CT regions 2, 3, and 4 but were much higher at the ultra-distal epiphysis (region 1 ~77 %). At the femur, BMD losses were comparable to those seen with pQCT (~70 %) only for the central sampled regions. CT-derived BMD losses were lower at the proximal and distal extremes of the femur. This contrasts with one recent study that reported maximum declines in BMD at the most distal limit of the femur [2]. Methodological differences in indexing the analysis segments to the "endpoint" of the femur may have contributed to this discrepancy.

Because the magnitude of osteoclastic activity in any given bone region is dependent upon the surface/volume ratio of the local trabecular elements [43], anatomic differences along the bone's length likely predispose some regions to excessive bone loss. As confirmation, BMD and architecture declines for participant 1 were universally lowest for the most proximal sampled tibia and femur segments. The marrow cavity begins to form near these regions, reducing the number of trabeculae available for osteoclastic activity, thereby reducing the longitudinal percentage loss of bone at these sites. The higher surface/volume ratio of the more distal epiphyseal regions creates ample space for osteoclastic activity, but by the same token, may also prime these regions for greater anabolic cellular activity. An important direction for future research will be to determine whether trabecular bone regions that experience the most severe bone loss are also most amenable to bone preservation through mechanical loading interventions. The CT imaging approach used in the present study is an ideal method for exploring this issue.

The application of imaging peel modes permitted a detailed examination of various concentric zones within the trabecular envelope. We are aware of no previous reports that have examined differences in bone loss among concentric zones of CT images. This approach is important for interpretation of the present vibration study and for the design of future studies as well. If subtle training-related adaptations occurred in one cross-sectional zone but not in the others, detection of the effect could be undermined because of averaging with nonresponsive zones. In the present study, the absence of significant training effects with any of the four peel methods bolsters our conclusion that vibration training did not trigger bone adaptation in this cohort. Future training studies will identify which concentric regions experience the most rapid bone loss post-SCI and whether they remain responsive to mechanical loading interventions. By eliminating non-responsive areas from analysis, future studies will be best positioned to detect even subtle training adaptations in trabecular microarchitecture.

The CT-derived longitudinal values obtained for participant 1 provide important context for future applications of high-resolution imaging for post-SCI bone. Prior to this investigation we could only theorize the direction and magnitude of post-SCI changes in micro-architectural parameters, particularly for the VTA-derived indices that used plate and rod characterization. A comparison of micro-architecture raw values for participant 1 with the untrained limbs of the vibration cohort (all individuals with chronic SCI) confirms that architecture degradation continues beyond 2.7 years post-SCI (see Figs. 2, 4, and 5). Interestingly, this study adds complexity to the debate surrounding the development of steady state bone status with chronic SCI. Several previous pQCT studies suggested that BMD loss eventually ceases between 4 and 8 years post-SCI [3, 32, 33]. pQCT data spanning 12 months for the present vibration cohort indicated likewise. However, CT imaging revealed that BMD and trabecular network length continued to decline in these individuals. For the femur, we were able to pinpoint the anatomical regions experiencing the most consistent decline: regions 2 and 3, spanning 4–8 % of femur length. CT imaging also gave us insight into the interplay between architecture loss and BMD loss. For these participants at this particular time post-SCI, NL was the only architectural parameter continuing to deteriorate in conjunction with BMD. Thus, the observed decline in BMD in these individuals may have been "driven" by a decline in NL, as opposed to a decline in

trabecular thickness, width, or other architectural parameters. We believe that it is likely that at earlier time post-SCI, BMD decline may instead correlate more strongly with the decline of other features of trabecular architecture.

Methodologic considerations

The results of the present study pertain to vibratory input at a particular combination of frequency, amplitude, and session volume and do not necessarily indicate that vibration training per se is an ineffective anti-osteoporosis strategy. Future work is necessary to conclusively determine whether this mode of mechanical input has osteo-regulatory potential in human participants.

As no physical correspondence exists between the location or thickness of pQCT and CT slices, direct comparison between BMD values for these techniques is not possible. The percentage peel applied to CT images appears to affect the sensitivity of this technique for detecting bone adaptations across time. For example, we observed that the 30 % peel generally detected 3 % more change across time than the peripheral peel. A future longitudinal study with a larger cohort is needed to examine this methodological consideration of high-resolution CT imaging.

Conclusions

Twelve months of vibration training did not preserve BMD or trabecular architecture in participants with chronic SCI. These results underscore the insensitivity of bone in long-term SCI to mechanical loading interventions, in particular to the "dose" of vibration administered in this study. Other modes of vibration training may yet be fruitful interventions for other subsets of the SCI population. A novel finding of the present study was evidence for continued loss of BMD and trabecular network length in long-term SCI, particularly in the most distal segments of the femur. A second novel finding was that a participant followed longitudinally from acute to chronic SCI showed spatial variation in BMD and architecture loss along the longitudinal axis of the femur and the tibia. Future work is needed to determine if the bone regions at greatest risk for deterioration after SCI may also respond most favorably to anti-osteoporosis interventions.

Acknowledgments

References

1. Qin W, Bauman WA, Cardozo CP. Evolving concepts in neurogenic osteoporosis. Curr Osteoporos Rep. 2010; 8:212–218. [PubMed: 20820963]

2. Edwards WB, Schnitzer TJ, Troy KL. Bone mineral and stiffness loss at the distal femur and proximal tibia in acute spinal cord injury. Osteoporos Int. 2014; 25:1005–1015. [PubMed: 24190426]

3. Dudley-Javoroski S, Shields RK. Regional cortical and trabecular bone loss after spinal cord injury. J Rehabil Res Dev. 2012; 49:1365–1376. [PubMed: 23408218]

4. Dudley-Javoroski S, Saha PK, Liang G, Li C, Gao Z, Shields RK. High dose compressive loads attenuate bone mineral loss in humans with spinal cord injury. Osteoporos Int. 2012; 23:2335–2346. [PubMed: 22187008]

5. Dudley-Javoroski S, Shields RK. Asymmetric bone adaptations to soleus mechanical loading after spinal cord injury. J Musculoskelet Neuronal Interact. 2008; 8:227–238. [PubMed: 18799855]

6. Dudley-Javoroski S, Shields RK. Active-resisted stance modulates regional bone mineral density in humans with spinal cord injury. J Spinal Cord Med. 2013; 36:191–199. [PubMed: 23809588]

7. Shields RK, Dudley-Javoroski S. Musculoskeletal plasticity after acute spinal cord injury: Effects of long-term neuromuscular electrical stimulation training. J Neurophysiol. 2006; 95:2380–2390. [PubMed: 16407424]

8. Hartkopp A, Murphy RJ, Mohr T, Kjaer M, Biering-Sorensen F. Bone fracture during electrical stimulation of the quadriceps in a spinal cord injured subject. Arch Phys Med Rehabil. 1998; 79:1133–1136. [PubMed: 9749697]

9. Kern H, Carraro U, Adami N, et al. Home-based functional electrical stimulation rescues permanently denervated muscles in paraplegic patients with complete lower motor neuron lesion. Neurorehabil Neural Repair. 2010; 24:709–721. [PubMed: 20460493]

10. Fritton SP, McLeod KJ, Rubin CT. Quantifying the strain history of bone: spatial uniformity and self-similarity of low-magnitude strains. J Biomech. 2000; 33:317–325. [PubMed: 10673115]

11. Garman R, Rubin C, Judex S. Small oscillatory accelerations, independent of matrix deformations, increase osteoblast activity and enhance bone morphology. PLoS ONE. 2007; 2:e653. [PubMed: 17653280]

12. Bramlett HM, Dietrich WD, Marcillo A, et al. Effects of low intensity vibration on bone and muscle in rats with spinal cord injury. Osteoporos Int. 2014

13. Ozcivici E, Garman R, Judex S. High-frequency oscillatory motions enhance the simulated mechanical properties of non-weight bearing trabecular bone. J Biomech. 2007; 40:3404–3411. [PubMed: 17655852]

14. Rubin C, Turner AS, Mallinckrodt C, Jerome C, McLeod K, Bain S. Mechanical strain, induced noninvasively in the high-frequency domain, is anabolic to cancellous bone, but not cortical bone. Bone. 2002; 30:445–452. [PubMed: 11882457]

15. Huang RP, Rubin CT, McLeod KJ. Changes in postural muscle dynamics as a function of age. J Gerontol A Biol Sci Med Sci. 1999; 54:B352–B357. [PubMed: 10496541]

16. Asselin P, Spungen AM, Muir JW, Rubin CT, Bauman WA. Transmission of low-intensity vibration through the axial skeleton of persons with spinal cord injury as a potential intervention for preservation of bone quantity and quality. J Spinal Cord Med. 2011; 34:52–59. [PubMed: 21528627]

17. Davis R, Sanborn C, Nichols D, Bazett-Jones DM, Dugan EL. The effects of whole body vibration on bone mineral density for a person with a spinal cord injury: a case study. Adapt Phys Act Q. 2010; 27:60–72.

18. Wuermser LA, Beck LA, Lamb JL, Atkinson EJ, Amin S. The effect of low-magnitude whole body vibration on bone density and microstructure in men and women with chronic motor complete paraplegia. J Spinal Cord Med. 2014

19. McHenry CL, Wu J, Shields RK. Potential regenerative rehabilitation technology: implications of mechanical stimuli to tissue health. BMC Res Notes. 2014; 7:334. [PubMed: 24894666]

20. Bala Y, Depalle B, Farlay D, Douillard T, Meille S, Follet H, Chapurlat R, Chevalier J, Boivin G. Bone micromechanical properties are compromised during long-term alendronate therapy independently of mineralization. J Bone Miner Res. 2012; 27:825–834. [PubMed: 22189833]

21. Rubin CD. Emerging concepts in osteoporosis and bone strength. Curr Med Res Opin. 2005; 21:1049–1056. [PubMed: 16004672]

22. Giangregorio L, Lala D, Hummel K, Gordon C, Craven BC. Measuring apparent trabecular density and bone structure using peripheral quantitative computed tomography at the tibia: precision in participants with and without spinal cord injury. J Clin Densitom. 2013; 16:139–146. [PubMed: 22981715]

23. Edwards WB, Schnitzer TJ, Troy KL. The mechanical consequence of actual bone loss and simulated bone recovery in acute spinal cord injury. Bone. 2014; 60:141–147. [PubMed: 24361670]

24. Edwards WB, Schnitzer TJ, Troy KL. Reduction in proximal femoral strength in patients with acute spinal cord injury. J Bone Miner Res. 2014

25. Kirshblum SC, Burns SP, Biering-Sorensen F, Donovan W, Graves DE, Jha A, Johansen M, Jones L, Krassioukov A, Mulcahey M, Schmidt-Read M, Waring W. International Standards for Neurological Classification of Spinal Cord Injury (Revised 2011). J Spinal Cord Med. 2011; 34:535–546. [PubMed: 22330108]

26. Dudley-Javoroski S, Shields RK. Longitudinal changes in femur bone mineral density after spinal cord injury: effects of slice placement and peel method. Osteoporos Int. 2009; 21:985–995. [PubMed: 19707702]

27. Saha PK, Xu Y, Duan H, Heiner A, Liang G. Volumetric topological analysis: a novel approach for trabecular bone classification on the continuum between plates and rods. IEEE Trans Med Imaging. 2010; 29:1821–1838. [PubMed: 20562041]

28. Wehrli FW, Ladinsky GA, Jones C, et al. In vivo magnetic resonance detects rapid remodeling changes in the topology of the trabecular bone network after menopause and the protective effect of estradiol. J Bone Miner Res. 2008; 23:730–740. [PubMed: 18251704]

29. Garman R, Gaudette G, Donahue LR, Rubin C, Judex S. Low-level accelerations applied in the absence of weight bearing can enhance trabecular bone formation. J Orthop Res. 2007; 25:732–740. [PubMed: 17318899]

30. Chang SH, Dudley-Javoroski S, Shields RK. Gravitational force modulates muscle activity during mechanical oscillation of the tibia in humans. J Electromyogr Kinesiol. 2011

31. Chang SH, Tseng SC, McHenry CL, Littmann AE, Suneja M, Shields RK. Limb segment vibration modulates spinal reflex excitability and muscle mRNA expression after spinal cord injury. Clin Neurophysiol. 2012; 123:558–568. [PubMed: 21963319]

32. Eser P, Schiessl H, Willnecker J. Bone loss and steady state after spinal cord injury: a cross-sectional study using pQCT. J Musculoskelet Neuronal Interact. 2004; 4:197–198. [PubMed: 15615125]

33. Frotzler A, Berger M, Knecht H, Eser P. Bone steady-state is established at reduced bone strength after spinal cord injury: A longitudinal study using peripheral quantitative computed tomography (pQCT). Bone. 2008; 43:549–555. [PubMed: 18567554]

34. Bauman WA, Spungen AM, Wang J, Pierson RN Jr, Schwartz E. Continuous loss of bone during chronic immobilization: a monozygotic twin study. Osteoporos Int. 1999; 10:123–127. [PubMed: 10501792]

35. Shields RK, Dudley-Javoroski S. Musculoskeletal adaptation in chronic spinal cord injury: effects of long-term soleus electrical stimulation training. J Neurorehabil Neural Repair. 2007; 21:169–179.

36. Frey Law L, Shields RK. Femoral loads during passive, active, and active-resistive stance after spinal cord injury: a mathematical model. Clin Biomech. 2004; 19:313–321.

37. McHenry CL, Shields RK. A biomechanical analysis of exercise in standing, supine, and seated positions: implications for individuals with spinal cord injury. J Spinal Cord Med. 2012; 35:140–147. [PubMed: 22507023]

38. Chilibeck PD, Bell G, Jeon J, Weiss CB, Murdoch G, MacLean I, Ryan E, Burnham R. Functional electrical stimulation exercise increases GLUT-1 and GLUT-4 in paralyzed skeletal muscle. Metabolism. 1999; 48:1409–1413. [PubMed: 10582549]

39. Gorgey AS, Mather KJ, Cupp HR, Gater DR. Effects of resistance training on adiposity and metabolism after spinal cord injury. Med Sci Sports Exerc. 2012; 44:165–174. [PubMed: 21659900]

40. Griffin L, Decker MJ, Hwang JY, Wang B, Kitchen K, Ding Z, Ivy JL. Functional electrical stimulation cycling improves body composition, metabolic and neural factors in persons with spinal cord injury. J Electromyogr Kinesiol. 2008; 19:614–622. [PubMed: 18440241]

41. Jeon JY, Hettinga D, Steadward RD, Wheeler GD, Bell G, Harber V. Reduced plasma glucose and leptin after 12 weeks of functional electrical stimulation-rowing exercise training in spinal cord injury patients. Arch Phys Med Rehabil. 2010; 91:1957–1959. [PubMed: 21112441]

42. Mahoney ET, Bickel CS, Elder C, Black C, Slade JM, Apple D Jr, Dudley GA. Changes in skeletal muscle size and glucose tolerance with electrically stimulated resistance training in subjects with chronic spinal cord injury. Arch Phys Med Rehabil. 2005; 86:1502–1504. [PubMed: 16003691]

43. Rittweger J, Goosey-Tolfrey VL, Cointry G, Ferretti JL. Structural analysis of the human tibia in men with spinal cord injury by tomographic (pQCT) serial scans. Bone. 2010; 47:511–518. [PubMed: 20561989]
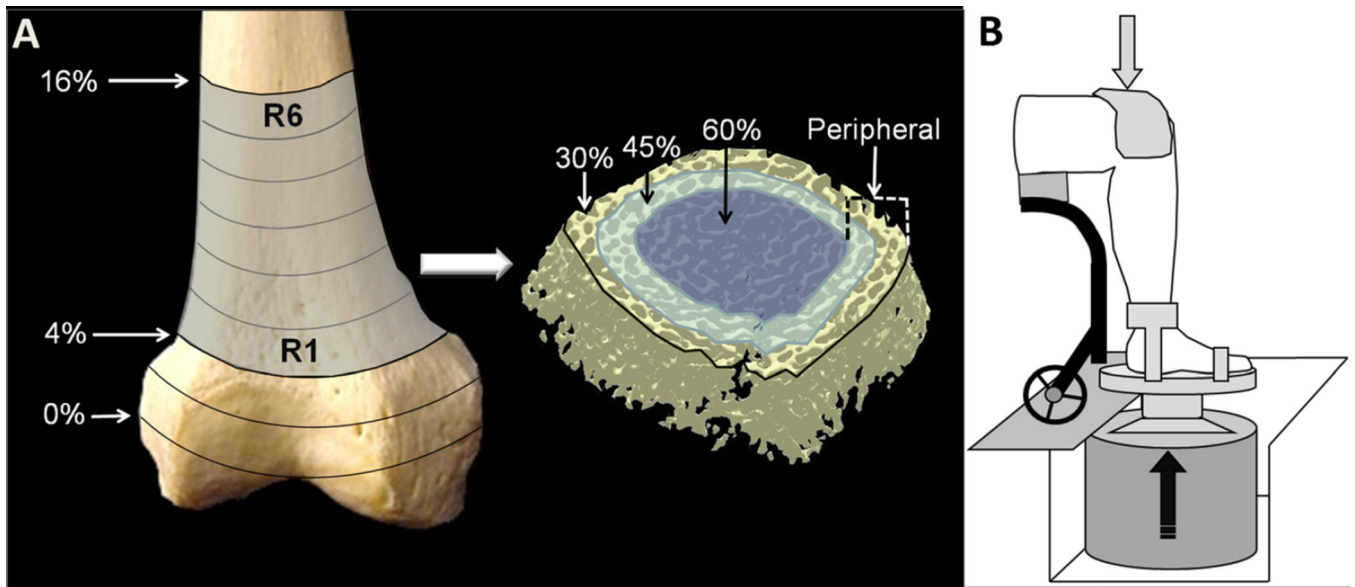
Fig. 1.

a Schematic representation of the computed tomography (CT) image-processing technique. For both the distal femur and the distal tibia, we analyzed six regions that spanned 4–16 % of the bone length (R1–R6). Each region was then processed with three concentric peel modes which removed external voxels corresponding to 30, 45, and 60 % of the region's cross-sectional area. The final peel mode (peripheral) analyzed the outermost ring of trabecular bone by subtracting the area delineated by the 60 % peel from the area delineated by the 30 % peel. Bone mineral density (BMD) and five trabecular architecture parameters were calculated for each peel mode for each bone region. **b** Schematic representation of the vibration training system. Ankle and forefoot straps secured the foot to the vibrating surface. To securely couple the limb segment to the vibrating surface, a compressive load of 10–15% of body weight was applied to the top of the knee via a full-contact pad. Technical details of the vibration system have been described elsewhere [19, 30, 31]
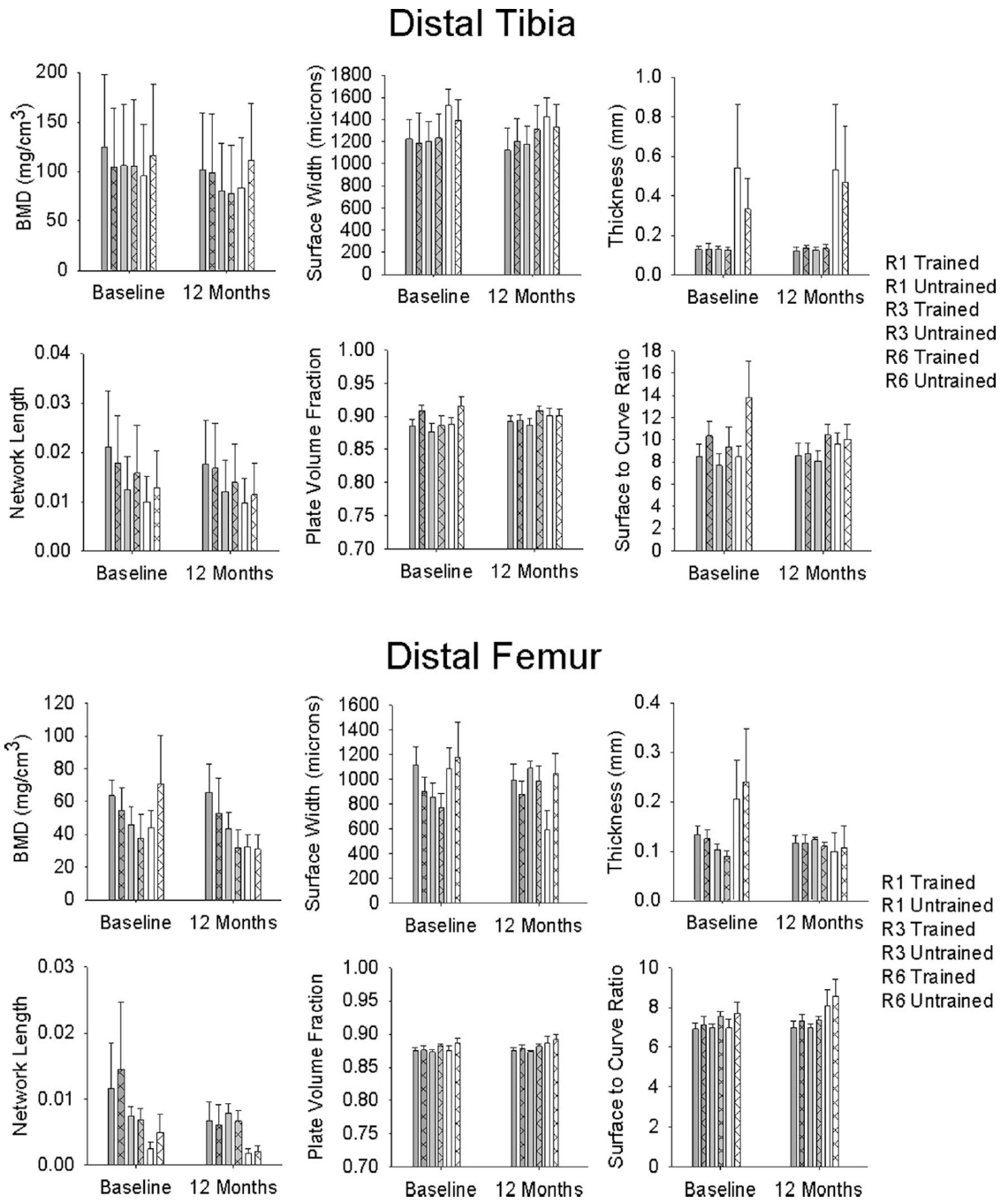
Fig. 2.
Mean/standard error computed tomography (CT)-derived bone mineral density (BMD) and trabecular architecture for the vibration training cohort at baseline and after 12 months of unilateral training. For clarity, representative CT regions are shown as described in Fig. 1 (R1, R3, and R6)
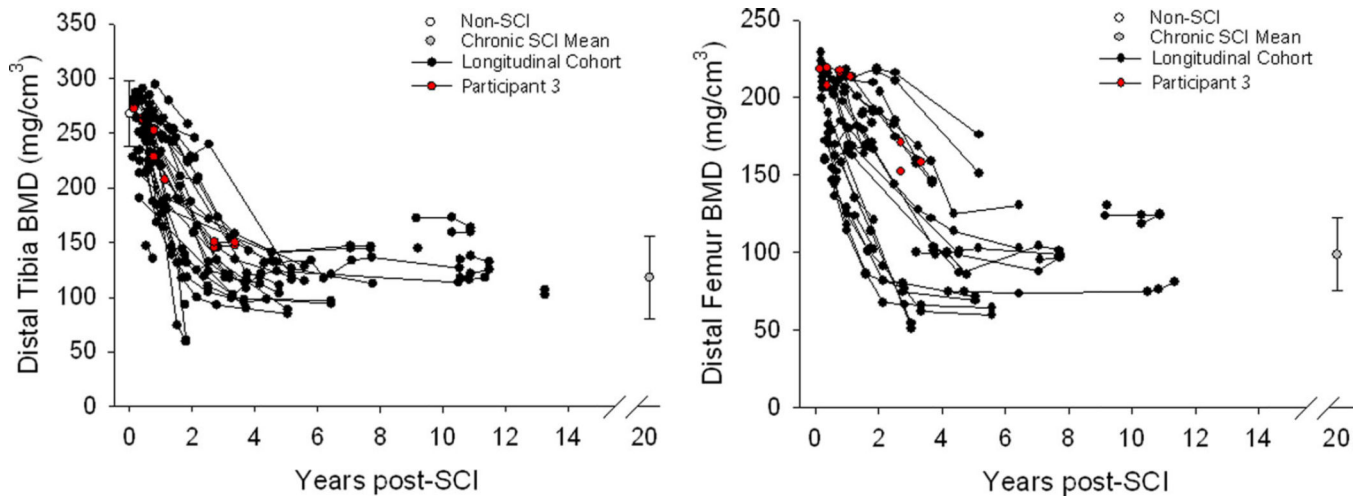
Fig. 3.
Peripheral quantitative computed tomography (pQCT)-derived bone mineral density (BMD) for participants with and without spinal cord injury (SCI), including the individual who was concurrently followed with computed tomography (CT) (participant 1). For clarity, data for individuals with SCI>15 years are pooled (*gray plot*). Data for this group and for non-SCI participants are shown as mean/standard error. Joint contractures and involuntary muscle spasms prevented some SCI participants from undergoing femur scans
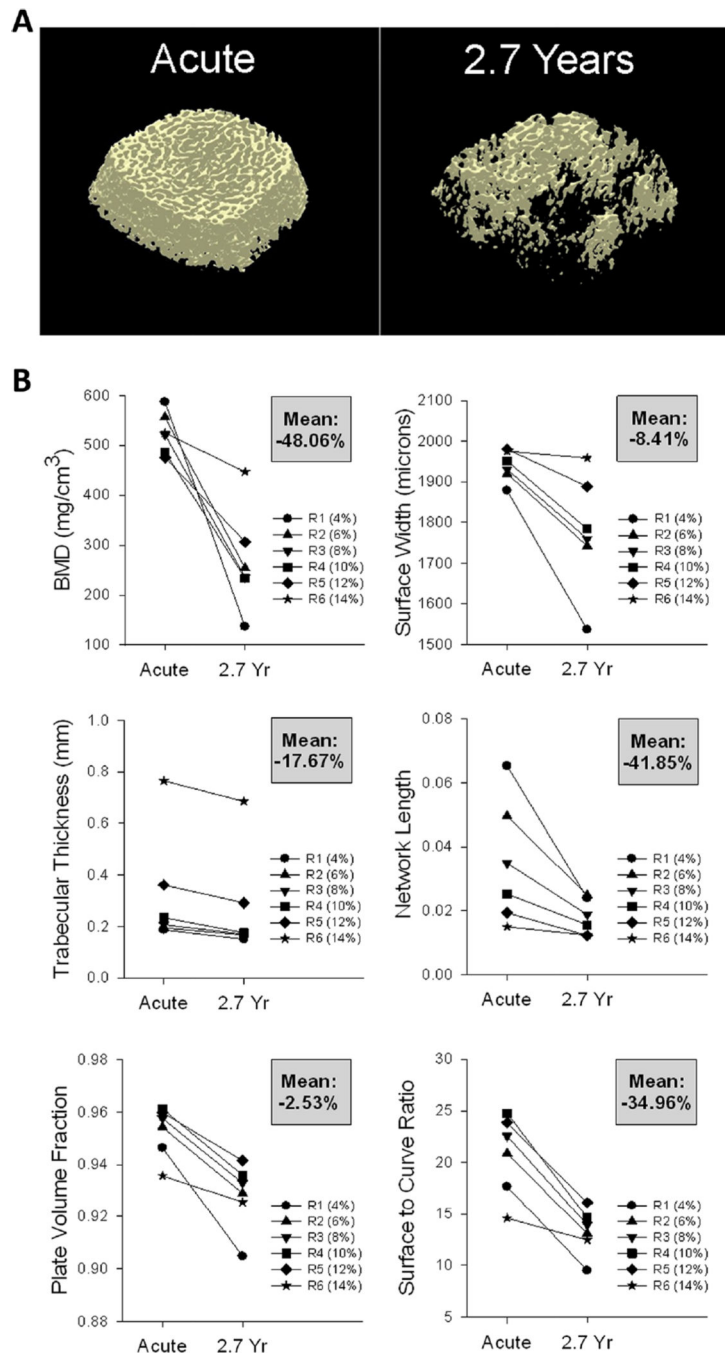
Fig. 4.

Computed tomography (CT) data for a participant followed longitudinally from acute to chronic spinal cord injury (SCI) (2.7 years). a Representative examples of CT images (30 % peel) from the right distal tibia. b Bone mineral density (BMD) and trabecular architecture values for each CT region (R1–R6). The mean percent change across time for all regions is shown in the *gray box* for each panel
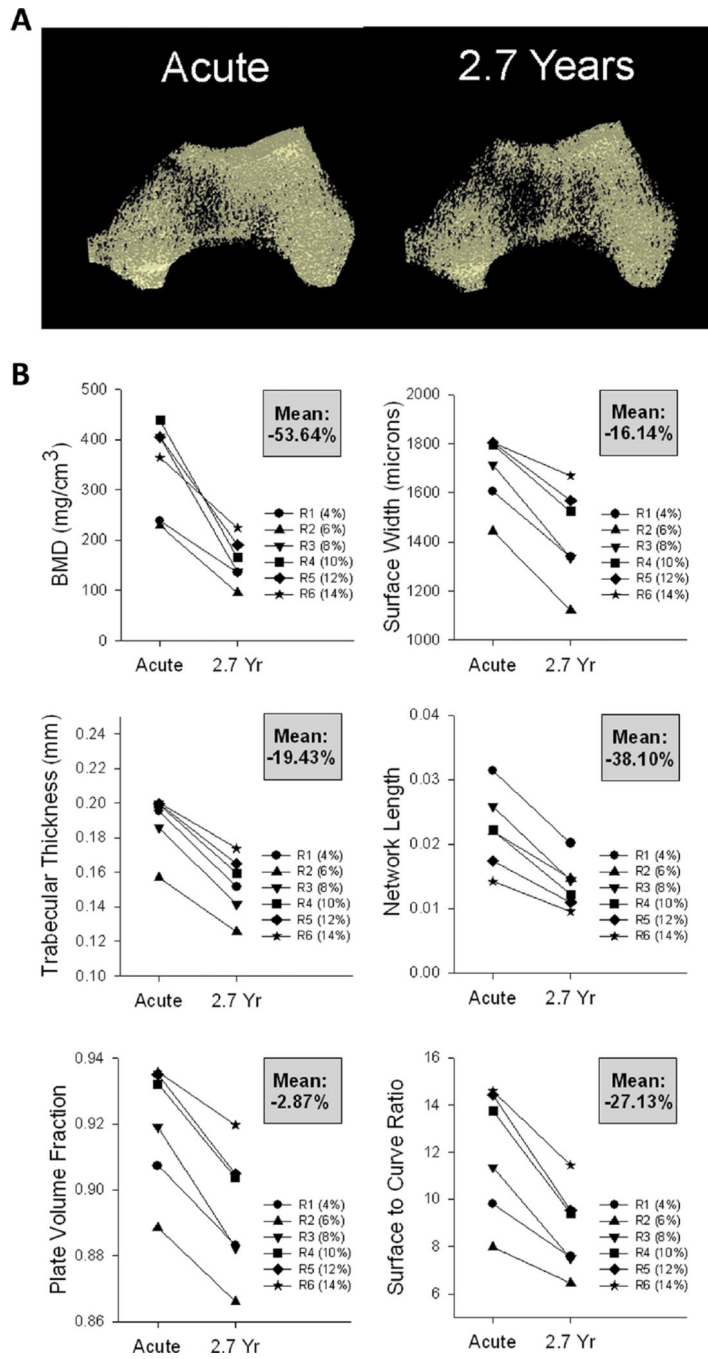
Fig. 5.

Computed tomography (CT) data for a participant followed longitudinally from acute to chronic spinal cord injury (SCI) (2.7 years). **a** Representative examples of CT images (30 % peel) from the right distal femur. **b** Bone mineral density (BMD) and trabecular architecture values for each CT region (R1–R6). The mean percent change across time for all regions is shown in the *gray box* for each panel.

Table 1

Demographic data

Participant	Gender	SCI level	AIS	Age	SCI years at first pQCT	Number of pQCTs	SCI years at first CT	Sessions completed	Sessions/week	Percent compliance
1	M	T4	A	17	0.14	6	0.36	N/A	N/A	N/A
2	M	T8	A	23	0.19	5	3.75	152	2.44	81.22
3	M	T7	A	29	0.30	6	4.36	148	2.22	74.16
4	M	T4	A	34	2.40	6	9.10	112	2.31	76.88
5	F	C7	B	66	9.15	3	9.15	116	2.14	71.25
6	F	T4	A	33	10.56	3	10.56	149	2.51	83.63
7	M	T8	B	65	16.65	3	14.73	147	2.23	74.30

Participant 1 was followed longitudinally via peripheral quantitative computed tomography (pQCT) and high-resolution computed tomography (CT) for the first 2.7 years post-spinal cord injury (SCI.)

Participants 2–7 completed >112 vibration sessions over 12 months, averaging >2.14 sessions per week (>76 % compliance)

AIS American Spinal Injury Association Impairment Scale, *N/A* not applicable